



An Tang<sup>1,2,3</sup>  
 Guy Cloutier<sup>2,3,4,5</sup>  
 Nikolaus M. Szeverenyi<sup>6</sup>  
 Claude B. Sirlin<sup>6</sup>

**Keywords:** elasticity, elastography, liver fibrosis, MR elastography (MRE), MRI, shear stiffness, shear wave, ultrasound, viscoelasticity, viscosity

DOI:10.2214/AJR.15.14552

Received February 17, 2015; accepted without revision February 19, 2015.

Based on a presentation at the Radiological Society of North America 2012 annual meeting, Chicago, IL.

Technologies developed by the team of G. Cloutier were licensed to Rheolution Inc. and Acist Medical System. This work was supported by the Canadian Institutes of Health Research, Institute of Nutrition, Metabolism, and Diabetes (grant nos. 273738 and 301520 to A. Tang), the Fonds de Recherche du Québec—Santé (Career Award no. 26993 to A. Tang), New Researcher Startup Grant from the Centre de Recherche du Centre Hospitalier de l'Université de Montréal (support to A. Tang), Canadian Institutes of Health Research (grant nos. MOP-84358 and CPG-95288 to G. Cloutier), the Natural Sciences and Engineering Research Council of Canada (grant no. CHRP-365656-09 to G. Cloutier), the Fonds Québécois de la Recherche sur la Nature et les Technologies (grant no. FQRNT PR-174387 to G. Cloutier), and U.S. National Institute of Diabetes and Digestive and Kidney Diseases (grant nos. R56DK090350 and R01DK088925 to C. B. Sirlin).

<sup>1</sup>Department of Radiology, Centre Hospitalier de l'Université de Montréal, Montréal, QC, Canada.

<sup>2</sup>Centre de Recherche du Centre Hospitalier de l'Université de Montréal, Montréal, QC, Canada.

<sup>3</sup>Department of Radiology, Radio-Oncology and Nuclear Medicine, Université de Montréal, Montréal, QC, Canada.

<sup>4</sup>Institute of Biomedical Engineering, Université de Montréal, Montréal, QC, Canada.

<sup>5</sup>Laboratory of Biorheology and Medical Ultrasonics, Centre hospitalier de l'Université de Montréal, Montréal, QC, Canada.

<sup>6</sup>Liver Imaging Group, Department of Radiology, University of California San Diego, 408 Dickinson St, San Diego, CA 92103-8226. Address correspondence to C. B. Sirlin (csirlin@ucsd.edu).

#### Supplemental Data

Available online at [www.ajronline.org](http://www.ajronline.org).

AJR 2015; 205:22–32

0361–803X/15/2051–22

© American Roentgen Ray Society

# Ultrasound Elastography and MR Elastography for Assessing Liver Fibrosis: Part I, Principles and Techniques

**OBJECTIVE.** The purpose of this article is to provide an overview of ultrasound and MR elastography, including a glossary of relevant terminology, a classification of elastography techniques, and a discussion of their respective strengths and limitations.

**CONCLUSION.** Elastography is an emerging technique for the noninvasive assessment of mechanical tissue properties. These techniques report metrics related to tissue stiffness, such as shear-wave speed, magnitude of the complex shear modulus, and the Young modulus.

Imaging-based elastography is an emerging technology that uses imaging to noninvasively assess mechanical tissue properties. Elastography techniques have evolved significantly over the last 2 decades and have now been implemented on clinical ultrasound and MR systems [1–4]. These techniques provide the capability to examine by imaging what once could be examined only by direct palpation, which is likely to open new opportunities to noninvasively diagnose disease, guide management, and improve outcomes.

In this first article of a two-part series (see part 2 elsewhere in this issue [5]), we provide a brief overview of elastography, including a glossary of commonly used terms (Table 1), a classification of techniques, a description of the basic principles, definitions of mechanical properties, examples of ultrasound and MR elastography, and a discussion of their respective strengths and limitations.

#### Key Learning Points

First, imaging-based elastography techniques have been developed to measure stiffness and other mechanical properties noninvasively for both research and clinical indications. In general, these techniques cannot measure stiffness directly; instead, they assess stiffness indirectly by measuring the speed of shear waves propagating in the tissue of interest. The underlying concept is that shear-wave speed is related to tissue stiffness: shear waves travel faster in stiff tissues and slower in soft tissues.

Second, by measuring shear-wave speed, ultrasound elastography and MR elastography

techniques estimate tissue stiffness. Depending on the technique, various stiffness-related parameters may be reported. The most commonly reported parameters and corresponding units are shear-wave speed in meters per second, magnitude of complex shear modulus in kilopascals (commonly described in the literature as “shear stiffness”), and the Young elastic modulus in kilopascals (commonly described in the medical literature as “elasticity”). The lack of uniformity in the reported parameters complicates comparisons across techniques. These elastography techniques may also measure parameters other than stiffness, including shear-wave attenuation and tissue viscosity, although these additional parameters are considered investigational and have not yet been reported clinically.

Third, shear waves may be generated by applying a mechanical vibration to the surface of the body or by focusing an acoustic radiation force (acoustic push pulse) inside the tissue of interest. Some ultrasound-based techniques use mechanical vibration for shear-wave generation, whereas others use acoustic radiation force. Commercial MRI-based techniques use only the former. The duration of the shear waves also is variable. Shear waves are generated transiently for ultrasound elastography and continuously for MR elastography.

Fourth, ultrasound elastography techniques track shear waves by using ultrasound-tracking beams. Some ultrasound-based techniques display parametric maps called “elastograms” that display the spatial distribution of the stiffness-related parameter of interest; others provide only numeric results.

## Ultrasound and MR Elastography of Liver Fibrosis

Finally, MR elastography tracks shear waves by acquiring images with wave motion-sensitized phase-contrast sequences. Tissue motion caused by the shear waves during the scan are encoded into the phase of the MR signal. This phase information is further processed to generate wave images depicting shear wave displacement

within the liver. Subsequent processing of the wave images produces elastograms.

### Classification

As summarized in Figure 1, elastography techniques may be classified according to the source (static, quasistatic, or dynamic) and duration

(transient or continuous) of tissue deformation and the modality used for tracking (ultrasound or MRI). Techniques also may be classified according to the device type (stand alone or adjunct to an imaging scanner), wave generation method (external vibrator or internally focused acoustic radiation force), in-

**TABLE 1: Glossary of Commonly Used Terms in Elastography**

Term	Definition
Acoustic radiation force impulse	Ultrasonic compression waves focused on a spot to create shear waves perpendicular to the ultrasound beam axis. Point shear-wave elastography and shear-wave elastography use acoustic radiation force impulses (also called acoustic push pulses) to generate shear waves. Acoustic radiation force impulse may also refer to a particular technique commercialized by Siemens Healthcare that includes both the wave-generation method and a proprietary wave-tracking method.
Attenuation	The loss in amplitude of waves through viscous tissue.
Compression wave	A type of wave in which oscillation motion is parallel to the direction of wave propagation; it is also known as P, primary, or longitudinal wave.
Complex shear modulus ( $G^*$ )	A measure of the overall resistance of a material to an applied shear stress; it has two components: an elastic component called the storage modulus, which is the real part of the complex shear modulus, and a viscous component called the loss viscous modulus, which is the imaginary part of the complex shear modulus.
Dynamic (shear) elastography	A type of elastography technique that relies on the production of shear waves and measurement of shear wave speed propagation.
Effective shear modulus ( $\mu$ )	A term used in the MR elastography literature to describe the resistance to deformation on application of a shear stress; it is related to the shear wave speed by the following equation: $\mu = \rho c^2$ , where $\mu$ is the effective shear modulus, $\rho$ is the density of the tissue, and $c$ is the shear wave speed.
Elastic (Young) modulus ( $E$ )	A measure of elasticity (springlike behavior); it indicates the ability of a material to resist normal (perpendicular) deformation.
Elasticity	A characteristic of materials that tend to return to their initial shape after a deformation.
Elastogram	A graphical display (parametric map) indicating the spatial distribution of stiffness or stiffness-related parameter.
Elastography	A field of medical imaging that displays or measures the mechanical properties of soft tissues.
Inversion algorithm	Mathematic algorithm that allows calculation of mechanical properties from wave images.
Kilopascal (kPa)	A unit of pressure (force per unit area); it is a measure of tissue stiffness in ultrasound elastography and MR elastography.
Loss (viscous) modulus ( $G''$ )	The imaginary part of the complex shear modulus; it describes the dashpot-like energy-absorbing and -damping behavior.
Point shear-wave elastography	An elastography technique that measures regional values of shear-wave speed using acoustic radiation force impulse; the prototype is acoustic radiation force impulse quantification.
Quasistatic elastography	A type of elastography technique that relies on measurement of tissue deformation that arises from cardiac or respiratory motion.
Shear stiffness	A term commonly used in the literature to describe the magnitude (absolute value) of the complex shear modulus.
Shear wave	A type of wave in which oscillation motion is perpendicular to the direction of wave propagation; it is also known as S, secondary, or transverse waves.
Shear-wave elastography	A term used to describe elastography techniques that generate images of shear-wave speed using excitations by acoustic radiation force; the prototype is supersonic shear imaging.
Static elastography	A type of elastography technique that relies on the measurement of tissue deformation before and after manual compression with a transducer.
Stiffness	A qualitative property that has traditionally been assessed through palpation. The concept of "stiffness" refers to resistance to deformation in response to an applied force; it is defined mathematically by numerous moduli (elastic, shear, bulk), each one describing the resistance to deformation of a material in response to different types of stresses or applied pressures: tensile forces, shear forces, and volumetric compressive forces, respectively.
Storage (shear) modulus ( $G'$ )	The real part of the complex shear modulus; it describes elasticity (springlike, energy-storing behavior)—that is, the ability of a medium to resist shear (parallel to the surface) deformation without energy loss.
Transient elastography	A term used to designate techniques that rely on shear waves of short duration; the prototype is FibroScan (Echosens).
Viscoelasticity	A characteristic of materials that exhibit both viscous and elastic behavior when undergoing deformation.
Viscosity	A characteristic of materials that resists movement or deformation. It applies to both viscous fluid or viscous tissues.
Wave amplitude images	A graphic display of shear wave propagation often represented as a cine loop.

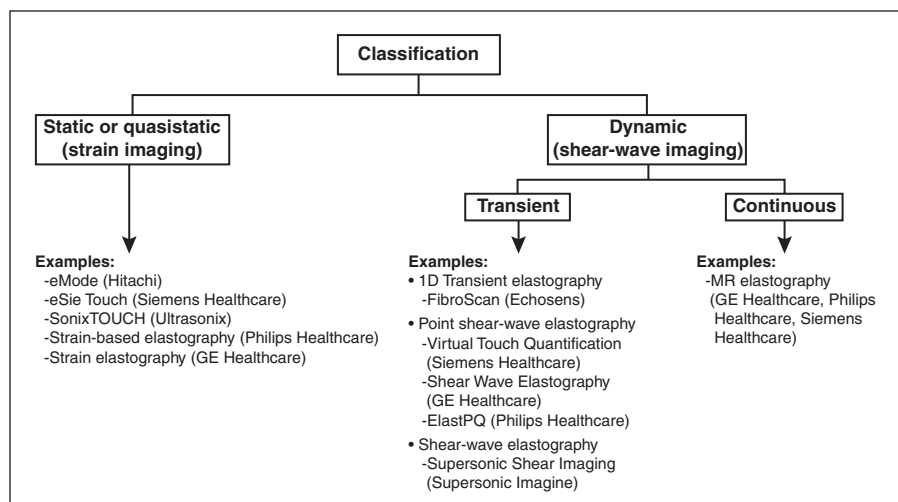


Fig. 1—Classification of elastographic techniques with focus on current commercial techniques.

version algorithm (1D, 2D, or 3D), reported parameters (shear-wave speed, magnitude of complex shear modulus, and the Young modulus), or output display (purely numeric, M-mode image, or parametric imaging map).

#### Static or Quasistatic Elastography

Static and quasistatic elastography assess stiffness by measuring the deformation (i.e., strain) in response to an applied force (i.e., stress) [6]. In static elastography, the stress is produced by manual compression of the tissue, whereas in quasistatic elastography, time-dependent stresses are produced by physiologic vibrations (e.g., the heart [7] or blood vessels [8]).

The assessment is qualitative, as opposed to quantitative, because the applied force cannot be known with certainty: manual compression in static elastography is operator dependent, and stresses caused by physiologic motion in quasistatic elastography are uncontrolled. Current static and quasistatic elastography techniques are ultrasound based. Static and quasistatic elastography will not be further discussed because of their limited applications for liver fibrosis.

#### Dynamic Elastography

Dynamic elastography techniques, also known as shear-wave imaging, assess stiffness and stiffness-related parameters by tracking shear waves propagating through media. Shear-wave speed is related to tissue stiffness; for instance, shear waves travel faster in stiff (inflamed, fibrotic, or cirrhotic) liver and slower in soft (normal or fatty) liver [9]. By measuring shear-wave speed, the stiffness may be inferred. For most biologic tissues, the shear-

wave speed and, hence, the inferred stiffness are frequency dependent: all other things being equal, shear-wave speed and inferred stiffness are greater if the shear waves are applied at higher frequency. Because the shear-wave frequencies used by different techniques differ, the stiffness-related values obtained with various techniques are not directly comparable.

#### Basic Principles

##### Types of Waves

Body waves, which travel inside organs, include compression and shear waves. With compression waves, tissue moves back and forth in a direction parallel to wave propagation. In contrast, shear waves produce tissue (particle) motion in a direction perpendicular to wave propagation [10]. Compression waves travel orders of magnitude faster than shear waves; in human soft tissues, compression waves propagate at around 1500 m/s, whereas shear waves propagate at around 1–10 m/s. Because compression waves propagate so rapidly through tissues, their speed and related properties cannot be reliably assessed by current imaging techniques. For this reason, all current imaging elastography techniques are based on tracking shear waves, not compression waves.

##### Wave Generation

Shear waves may be generated by either applying external mechanical vibration to the surface of the body or focusing acoustic radiation force impulses inside the tissue of interest. Some ultrasound-based techniques use the former method of shear wave generation, whereas others use the latter. MRI-based techniques use only mechanical vibration.

With ultrasound- and MRI-based external mechanical vibration techniques, the vibrator typically oscillates perpendicular to the body surface at a precisely controlled frequency. Compression waves are applied to the body surface; some of the energy in these compression waves is converted to shear waves through a process called mode conversion [11]. With external vibration, the shear-wave frequency can be controlled precisely and the associated energy absorption by tissue is minimal, but wave delivery into the tissue of interest may be inefficient.

With ultrasound-based acoustic radiation force techniques, acoustic compression pulses are focused inside the liver; some of the acoustic energy is absorbed and released in the form of shear waves [12]. Thus, shear waves are generated locally within the liver, which improves the efficiency of wave delivery into the area of interest. Compared with external vibration-induced waves, however, internally focused acoustic radiation forces are associated with higher power output and greater energy absorption, and the shear-wave frequency is more difficult to control.

#### Key Concepts of Dynamic Elastographic Examination

Regardless of the technique, dynamic elastography generally requires the following steps: baseline imaging, generation of shear waves, tracking of shear waves, and measurement of shear-wave speed or other mechanical parameter of interest.

#### Mechanical Properties and Parameters

Current clinically available techniques report the shear-wave speed, the magnitude of the complex shear modulus, or the Young modulus. The modulus parameters are often referred to as “stiffness” in the medical elastography literature, but strictly speaking do not have exactly the same meaning as stiffness, which is a qualitative property assessed through palpation. The term “stiffness” is permanently embedded in the medical elastography literature, however, and to maintain consistency with that literature, we also use the term to describe elastography measurements that approximate tissue response to palpation. Two such elastography parameters are elasticity and viscosity. Elasticity is the characteristic of a material that tends to return to its initial shape after a deformation. Viscosity is the characteristic of a material that resists rapid movement or deformation. Biologic tissues are considered to be visco-

**TABLE 2: Dynamic Elastography Techniques**

Modality, Implementations	Brand Name (Manufacturer)	Shear Wave				Parameter (Units)
		Generation	Duration	Frequency	Imaging	
Ultrasound						
1D Transient elastography	FibroScan (Echosens)	Mechanical	Transient	50 Hz	No anatomic image	Young elastic modulus (kPa)
Point shear-wave elastography	Virtual Touch Quantification (Siemens Healthcare)	Ultrasound (acoustic radiation force impulse)	Transient	Variable and difficult to precisely control	Location of ROI overlain on 2D B-mode image	Shear-wave speed (m/s)
Shear-wave elastography	Shear Wave Elastography (Supersonic Imagine)	Ultrasound (multipoint focalization of acoustic radiation force impulse)	Transient	Variable and difficult to precisely control	Quantitative elastogram within 2D image, with possibility to superimpose ROI	Young elastic modulus (kPa)
MRI						
MR elastography	MR Elastography (GE Healthcare, Philips Healthcare, Siemens Healthcare)	Mechanical	Continuous	60 Hz	Quantitative elastogram of one or more 2D slices <sup>a</sup>	Magnitude of complex shear modulus (kPa)

<sup>a</sup>Not all stiffness data are valid on the 2D elastogram. Valid data are considered reliable on the basis of confidence map and with good wave propagation.

**TABLE 3: Terminology Proposed by European Federation of Societies for Ultrasound in Medicine and Biology (EFSUMB) to Describe Ultrasound-Based Dynamic Elastography Techniques**

Term	Definition
1D transient elastography	Refers to methods that use a single-element ultrasound transducer to track shear waves generated externally by a vibrating probe placed on the body surface. The prototype is FibroScan developed by Echosens [17]. This is a stand-alone device without anatomic imaging capability. Some investigators refer to it as vibration-controlled transient elastography (VCTE).
Point shear-wave elastography	Refers to methods that measure shear-wave speed (or derived stiffness-related parameter) in a user-defined small ROI. Although a parametric map is not generated, the location of the ROI is captured on a conventional B-mode image. The prototype is Virtual Touch Quantification, using acoustic radiation force impulse technology commercialized by Siemens Healthcare [12].
Shear-wave elastography	Refers to methods that generate quantitative parametric maps displaying the shear-wave speed (or derived stiffness-related parameter). The prototype is Supersonic Shear Imaging developed by SuperSonic Imagine [34].

elastic, meaning that they have both viscous and elastic properties.

Investigational techniques may also calculate other parameters, but these additional measures are currently not reported in clinical settings. A full discussion of the numerous parameters is beyond the scope of this review. A brief summary is provided in the data supplement and Table S1, which both can be viewed in the *AJR* electronic supplement to this article, available at [www.ajronline.org](http://www.ajronline.org).

**Elastography Techniques**

Current elastography techniques are compared in Table 2 and illustrated in Figure 2.

**Ultrasound-Based Dynamic Elastography**

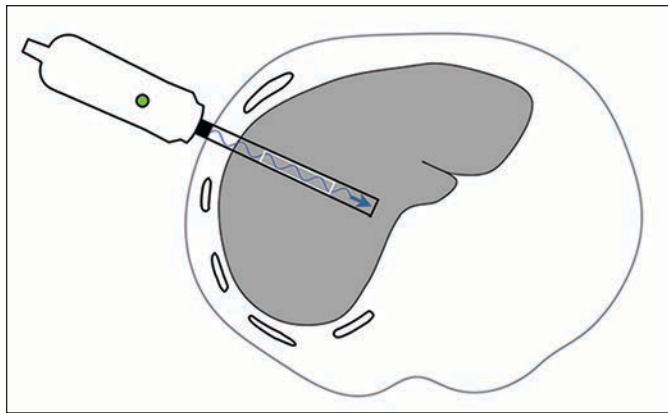
All current ultrasound-based dynamic elastography techniques use transient shear-wave excitations at a frequency of 50–400 Hz depending on the technique [2, 13, 14]. Numerous ultrasound-based techniques have become commercially available. To describe these techniques, we have adopted the terminology proposed by the European Federation of Societies for Ultrasound in Medicine and Biology [15], as summarized in Table 3.

*One-Dimensional Transient Elastography*

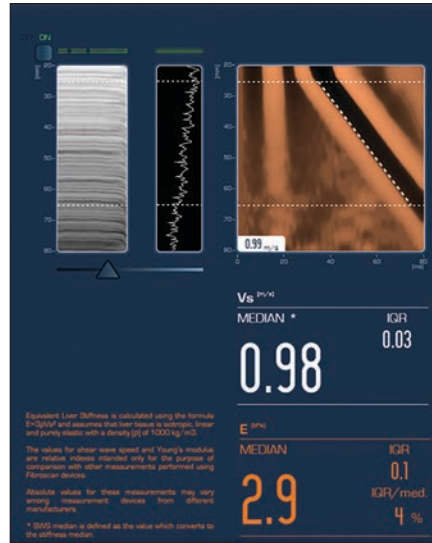
The first ultrasound-based shear-wave measurement technique based on the con-

cept of transient elastography was commercialized as FibroScan (Echosens). A single-element pistonlike ultrasound transducer mounted on a vibrating actuator generates a transient vibration (“punch”) of short duration (< 30 ms) [16] at a frequency of 50 Hz. The mechanical impulse generates a shear wave that propagates symmetrically with respect to the axis of the single-element transducer [2, 16–20]. The displacements induced by the shear wave are tracked using ultrasonic waves emitted and received at very high frequency (6 kHz) by the single-element ultrasound transducer. A compression wave is also produced by the mechanical impulse, but because of its high speed, it moves beyond the location at which the shear waves are tracked and does not interfere with the shear-wave measurements.

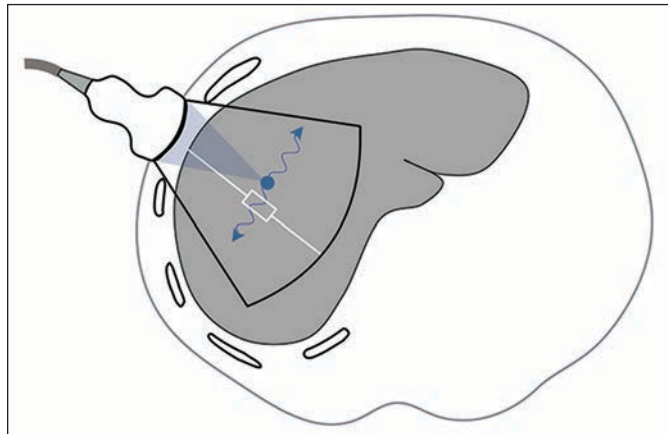
Ultrasound transducers are available targeted for pediatric (S1 and S2), nonobese adult (M), and obese adult (XL) patients. The S probes (S1 and S2) use a pulse-tracking frequency of 5 MHz at window depths of 15–40 mm and 20–50 mm, respectively [21]. The M probe uses a pulse-tracking frequency of 3.5 MHz at a window depth of 20–60 mm, and the XL probe uses a lower pulse-tracking frequency of 2.5 MHz at a window depth of 35–75 mm [19, 22]. The transient elastography device does not provide an anatomic image but instead provides M-mode and A-mode graphs to locate the optimal measurement point. The shear-wave propagation graph (Figs. 2A and 2B) is displayed after each acquisition. The acquired data are used to mea-



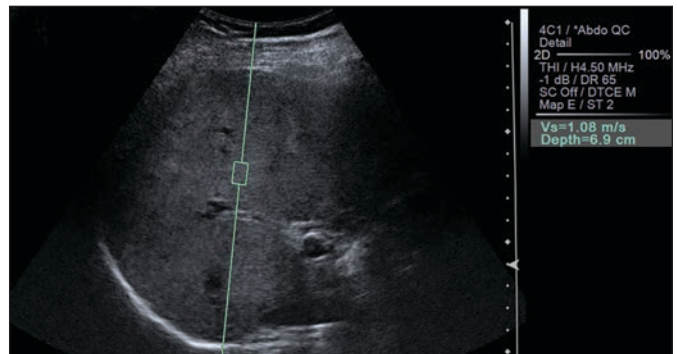
A



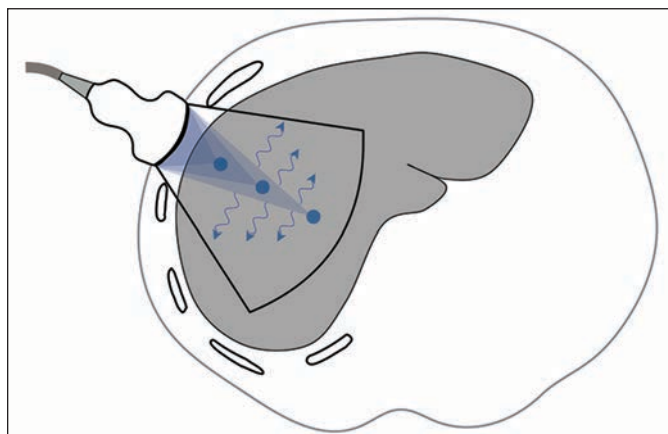
B



C



D



E



F

**Fig. 2**—Current elastography techniques.

**A–H**, Illustrations (**A**, **C**, **E**, and **G**; all by Tang A) show probe location, source of shear-wave generation (*blue arrows*), direction of shear-wave propagation, and FOV (*black outline*). Also shown are companion images (**B**, **D**, **F**, and **H**) produced by each elastography technique: 1D transient elastography (**A** and **B**; FibroScan image [**B**] courtesy of Echoscens), point shear wave elastography (**C** and **D**), shear-wave elastography (**E** and **F**), and MR elastography (**G** and **H**).

(Fig. 2 continues on next page)

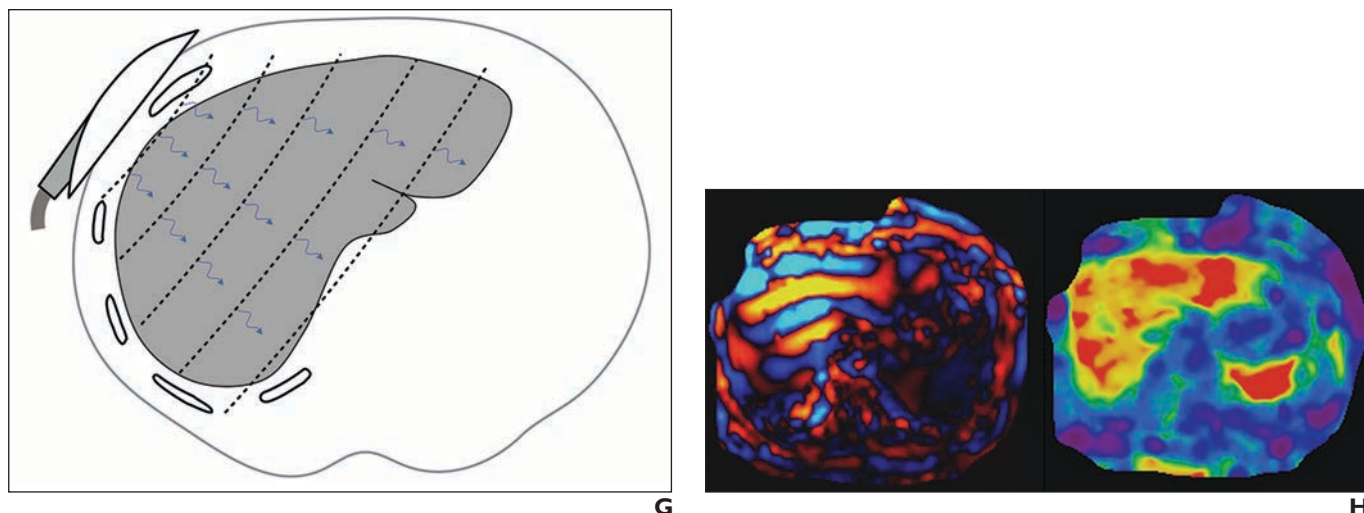


**Fig. 2 (continued)**—Current elastography techniques.

**A–H,** Illustrations (**A, C, E,** and **G;** all by Tang **A**) show probe location, source of shear-wave generation (*blue arrows*), direction of shear-wave propagation, and FOV (*black outline*). Also shown are companion images (**B, D, F,** and **H**) produced by each elastography technique: 1D transient elastography (**A** and **B;** FibroScan image [**B**] courtesy of Echosens), point shear wave elastography (**C** and **D**), shear-wave elastography (**E** and **F**), and MR elastography (**G** and **H**).

sure the shear-wave speed in the examined area. The results are converted to the Young modulus and reported in kilopascals. The M probe was the first to be available commercially and there is more extensive experience with this probe than the others.

**Advantages**—The technique is relatively inexpensive, highly portable, and widely available, and it has been independently validated in numerous centers worldwide. The instrument is easy to learn and the measurement is highly standardized and rapid to perform. For these reasons, it can be used by clinicians at the point of service, which is a major advantage [23]. Young modulus thresholds using the M-probe have been proposed for different causes of chronic liver disease, which facilitates interpretation of results [24]. The shear-wave frequency is controlled at 50 Hz, which ensures comparable measurements. The power output is low because the shear wave is generated mechanically, and there is little energy absorption by tissues.

**Limitations**—The technique may be limited in patients with obesity, narrow intercostal space, and ascites. The failure rate is lower with the XL probe than with the M probe (1.1% vs 16%) and reliability is higher (73% vs 50%) [25]. However, the performance of 1D transient elastography with the XL probe in obese subjects is controversial, with some studies reporting unreliability and failure rates as high as 23% [26, 27] and others as low as 6% [28]. This is problematic because obesity-associated fatty liver disease is emerging as the most common

cause of chronic liver disease in Western nations. Other elastography techniques also can be challenging in obesity [29]. Further research is required to better understand the performance of all elastographic techniques in the obese population. Although the various probes produce similar results in phantoms, the XL probe provides lower stiffness estimates than the M probe in humans [25, 30]. A plausible explanation is that different ROIs (window depths) are being measured and that, in obese patients, the region examined by the M mode may include subcutaneous tissues, which causes the stiffness to be overestimated. Regardless, stiffness thresholds for staging liver fibrosis reported with the M probe may not be directly applicable to the XL probe [30]. Because anatomic images are not captured, the exact measurement location is not recorded, which may introduce sampling variability for monitoring changes in stiffness over time. Without the imaging capability, the device has narrow applications beyond liver examination.

#### Point Shear-Wave Elastography

Point shear-wave elastography relies on a high-frequency spheric compression wave (acoustic radiation force impulse or acoustic push pulse) focused on a spot [12], which is then absorbed as acoustic energy. The absorbed acoustic energy causes the tissue to expand [31], which creates shear waves perpendicular to the ultrasound beam axis [1]. The shear-wave displacement created by the push pulse is recorded by a 2D ultrasound probe us-

ing a series of tracking pulses. From these data, the shear-wave speed can be derived. There are several implementations of point shear-wave elastography. These can be integrated onto existing ultrasound imaging scanners by adding the needed hardware (appropriate transducers and electronic components) and software (shear wave-tracking algorithms).

On the commercial Acuson S2000 and S3000 systems (Siemens Healthcare), acoustic radiation force impulses are implemented for qualitative (not further discussed) and quantitative applications. With the quantitative technique (Virtual Touch Quantification, Siemens Healthcare), a rectangular ROI (10 × 6 mm) is placed on a B-mode anatomic image (Figs. 2C and 2D). A transient shear wave is generated within the region. The shear wave is tracked and its speed measured. Results are reported as shear-wave speed in meters per second, at a range of 0.5–5 m/s in abdominal applications [32].

**Advantages**—This technique permits selection by the operator of an ROI in a representative area of the liver. The ROI is saved and, in principle, an ROI in a similar location could be selected in follow-up studies to permit more reliable monitoring. Point shear-wave elastography techniques are more robust than 1D transient elastography because shear waves are produced locally inside the liver and can be transmitted even in patients with a large body habitus or ascites. Although an entire ultrasound scanner may be more expensive than a 1D transient elastography device, the incremental cost of adding

the required software to an existing scanner is low.

**Limitations**—More expertise is needed than with 1D transient elastography. A radiologist or sonographer usually is required, and the technique is less suitable for point of service. Point shear-wave elastography is less validated than 1D transient elastography and currently is available on fewer scanners. Nevertheless, there are sufficient publications for a pooled meta-analysis on the diagnostic performance of point shear-wave elastography for staging of liver fibrosis [33]. The shear wave frequency is difficult to control precisely, which may introduce variability in measurements between different probes and manufacturers. Compared with 1D transient elastography, there is greater energy absorption by tissue.

### Shear-Wave Elastography

The Supersonic Shear Imaging technique (Aixplorer) combines a cone-shaped quasi-planar wave front and an ultrafast imaging technique to track shear-wave displacements across an entire imaging plane [34]. An acoustic radiation force is focused at successively greater depths on an axial line to produce multiple sequential spheric wave fronts. These interfere constructively to create a Mach cone with greater displacement magnitudes than those produced by the individual wave fronts. By analogy with supersonic planes, the Mach cone is produced because the rate of sequential wave front production is greater than the speed of the resulting shear waves. In the commercial implementation of shear-wave elastography, several Mach cones are produced at different lateral positions of the image. An

ultra-high frame rate (up to 15,000 images per second) is used to scan the entire imaging plane in one acquisition with high temporal resolution [13]. The combination of Mach cone generation and fast imaging allows real-time generation of elastograms. The results are reported as meters per second or converted to the Young modulus in kilopascals.

**Advantages**—This technique, which also relies on acoustic radiation force to generate shear waves, has similar strengths as point shear-wave elastography. Fast imaging permits generation of quantitative elastograms. Multiple ROIs then can be positioned on the elastograms, thereby reducing some of the sampling variability that can occur with 1D transient elastography and point shear-wave elastography [35].

**Limitations**—Shear-wave elastography has the same limitations as point shear-wave elastography with regard to the use of acoustic radiation force impulses. Compared with transient elastography and point shear-wave elastography, shear-wave elastography has restricted product availability, and, currently, there are fewer studies on its diagnostic performance for assessment of liver fibrosis [13, 36, 37].

### Newer Ultrasound-Based Systems

GE Healthcare and Philips Healthcare just released commercial shear-wave elastography packages for some of their imaging systems. These use acoustic radiation force to generate transient shear waves. Other manufacturers are following suit.

### MR Elastography

MR elastography has been implemented on 1.5- and 3-T clinical scanners. The

measured stiffness does not depend on field strength [38] but, as discussed earlier, does depend on mechanical excitation frequency [39]. Hence, mechanical properties acquired at different field strengths should be comparable as long as they are obtained with the same mechanical excitation frequency.

Because the spatial encoding of the shear-wave data is done over multiple wave cycles, MR elastography usually cannot measure transient shear waves. Instead, MR elastography techniques use continuous waves. MR elastography requires five components: a driver system to generate oscillatory mechanical waves continuously at a fixed frequency, a phase-contrast multiphase pulse sequence with motion-encoding gradients that are synchronized to the mechanical waves, processing of phase-sensitive MR images to depict wave amplitudes (shear-wave displacement images or, simply, wave images), further postprocessing (using an inversion algorithm) to generate elastograms (Fig. 3), and analysis of the elastograms.

### Driver System

Several driver systems have been designed to produce shear waves for MR elastography [40], including pneumatic, electromagnetic, piezoelectric, and focused ultrasound systems. The current commercial system is an acoustic driver with two components, an active and a passive driver: the active driver in the equipment room generates compression waves, which are transmitted through a flexible tube to the passive driver positioned against the right anterior chest wall of the subject in the scan room and secured using an elastic band. The passive driver usually is made of plastic and contains a flexible membrane that trans-

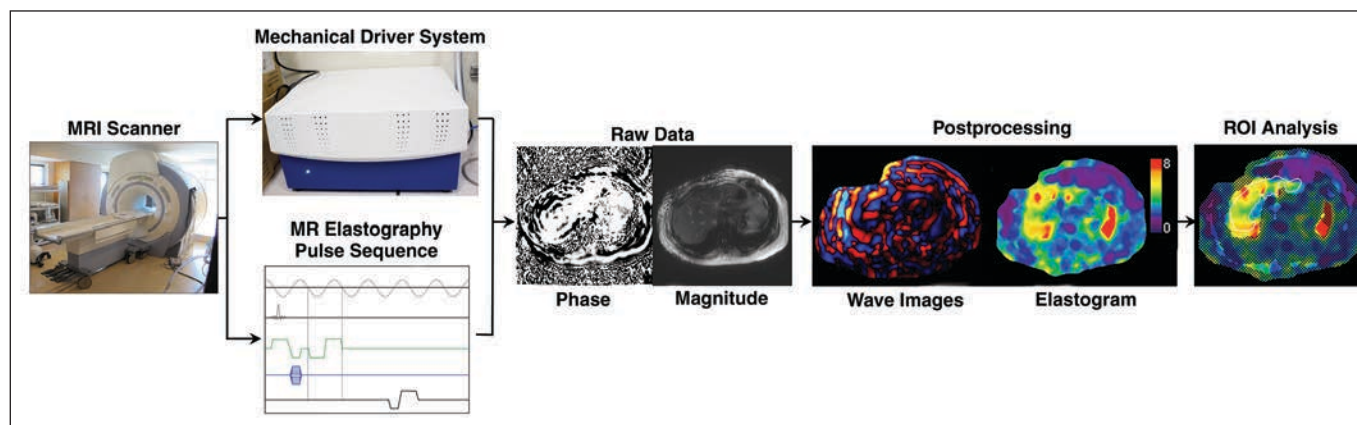


**Fig. 3**—MR elastography experiment works on clinical MRI scanners and requires five components: driver system to generate mechanical waves, phase-contrast multiphase pulse sequence with motion-encoding gradients that are synchronized to mechanical waves, acquisition of phase-sensitive MR images that contain raw data on wave motion and can also provide anatomic images, postprocessing to generate wave images and stiffness maps (also known as elastograms), and ROI analysis to produce single stiffness value. (Photographs by Tang A)

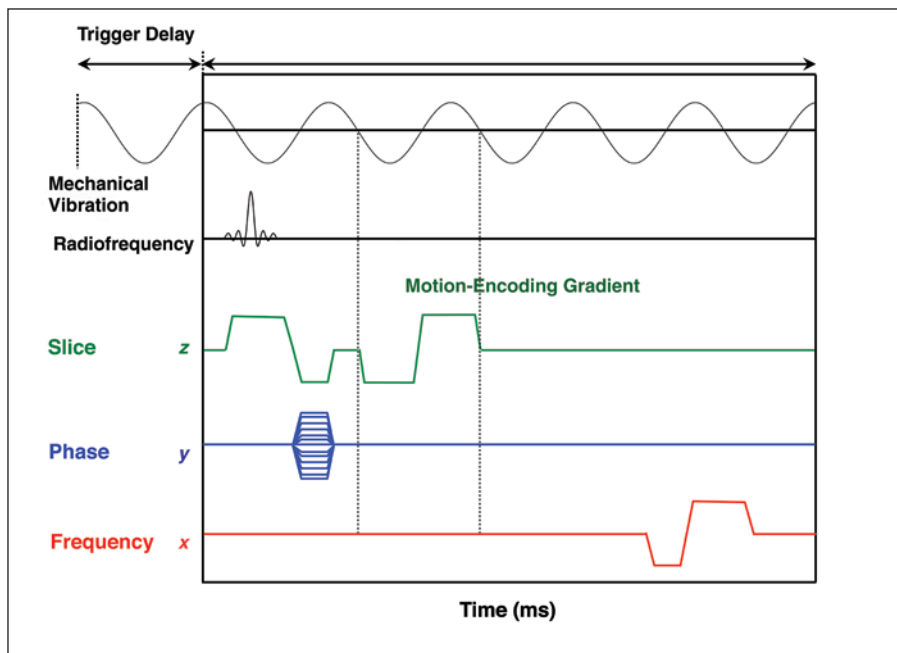


**Fig. 4**—Generic MR elastography sequence. Trigger pulse synchronizes mechanical vibration and motion-encoding gradient. In this diagram, motion-encoding gradient is applied using slice-select gradient. Motion-encoding gradients are applied successively in *x*, *y*, and *z* directions (when generating data for 3D inversion) and switched in polarity. In this diagram, frequency of motion-encoding gradient matches frequency of cyclic mechanical vibrations. Varying trigger delay shifts phase of mechanical wave relative to pulse sequence (motion-encoding gradient), allowing generation of data that capture propagation of wave displacements and that can be played as cine loop. Typically, four phase offsets are applied. Interpolation is applied to double number of phase offsets, from four to eight wave images to generate fluid cine loop.

mits the compression waves into the patient. The active driver does not need to be MRI compatible. These compression waves are then converted inside the patient’s body to shear waves by mode conversion.

In MR elastography, compression waves are generated continuously throughout the entire pulse sequence. The frequency used is typically around 60 Hz, because this low-frequency range results in waves with better propagation than higher-frequency waves while still yielding measurable shear wavelengths ranging from millimeters to centimeters [41].

**Pulse Sequence**

Various motion-sensitized MRI sequences, including gradient-recalled echo [4], spin-echo [42], echo-planar imaging [39, 43], and steady-state free precession [44], may be used to track the shear waves traversing the tissue of interest. A trigger pulse keeps the motion-encoding gradient synchronized with the compression waves generated by the driver. In most implementations, the frequency of the motion-encoding gradients matches the frequency of the waves. In the commercial 2D MR elastography sequence, the motion-encoding gradient is only applied in the *z* direction (orthogonal to

the patient axial plane), which suffices for 2D inversion of the wave component propagating along the *x*-*y* plane. In investigational 3D MR elastography sequences, motion-encoding gradients are successively applied in the *x*, *y*, and *z* directions. A generic MR elastography pulse sequence diagram designed to detect the propagation of shear waves is illustrated in Figure 4.

**Image Acquisition**

Images are acquired with a modified phase-contrast technique that generates both

magnitude and phase images. Because the motion-encoding gradients are synchronized with the frequency of the shear waves (phase locked), tiny particle displacements caused by the shear waves can be detected on the phase image. To acquire snapshots of the shear-wave propagation, phase images are acquired at different time offsets between the motion sensitization gradients and the shear waves (called phase offsets). Typically, four phase offsets are acquired (although 3D inversion techniques in development, as described later, use three phase offsets) to sample different spatial displacements of the wave cycle. Images at each phase offset are acquired through the liver at several slice locations to sample different portions of the liver. The total acquisition time is about 1 minute, typically divided into four separate approximately 15-second breath-holds (one for each slice location), acquired in end expiration if possible.

**Postprocessing**

The source phase images are postprocessed to produce wave displacement images. A mathematic filter called the curl filter separates the compression from the shear-wave components. In the clinical implementation adopted by MRI vendors, four additional phase offsets are interpolated to double the number of phase offset steps at each level to produce a fluid cine loop with eight wave images. Color maps are typically applied to these wave images, in which red and blue hues indicate opposite wave polarity and color saturation indicates wave amplitude.

These wave images are further processed to create elastograms, which depict the magnitude of the complex shear modulus. Waves propagate in three dimensions. The conversion from shear-wave displacement imag-

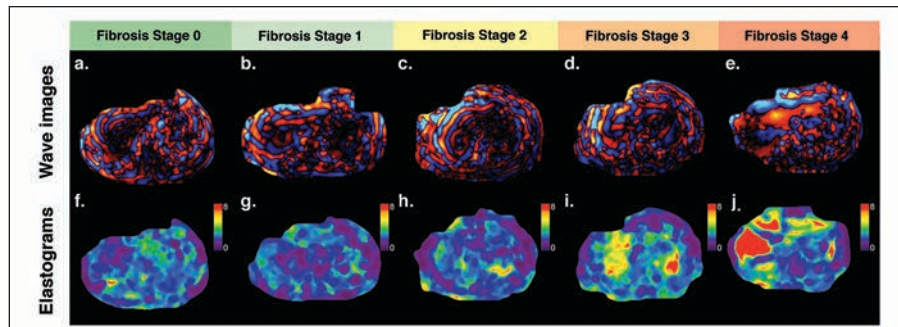


**Fig. 5**—MR elastography in different subjects correlated with biopsy-documented fibrosis stages. **A–J**, Axial wave cine loops (**A–E**) and corresponding axial elastogram images (**F–J**) are shown for subjects with fibrosis stages 0–4. Color elastogram represents magnitude of complex shear modulus with scale from 0 to 8 kPa.

**TABLE 4: Strengths and Limitations of Ultrasound Elastography and MR Elastography Techniques for Staging of Liver Fibrosis**

Modality, Implementations	Strengths	Limitations
Ultrasound		
1D transient elastography	<p>Relatively inexpensive</p> <p>Highly portable</p> <p>Widely available</p> <p>Independently validated worldwide</p> <p>Used by clinicians at point of service</p> <p>Shear-wave frequency controlled at 50 Hz</p> <p>Little energy absorption by tissues</p>	<p>Failure and unreliable results due to obesity, narrow intercostal space, ascites</p> <p>Potential classification discrepancies between M, XL, and S probes</p> <p>No anatomic images captured</p> <p>No recording of exact measurement location</p> <p>Narrow applications outside of liver investigation</p>
Point shear-wave elastography	<p>Permits selection of an ROI on B-mode ultrasound images</p> <p>ROI is saved and may be selected in follow-up studies to permit reliable monitoring</p> <p>Point shear-wave elastography more robust than 1D transient elastography</p> <p>Generates shear waves inside the liver (more robust)</p> <p>Diagnostic performance similar to that of 1D transient elastography</p> <p>Low incremental cost of adding required software to an existing scanner</p>	<p>More expertise required than 1D transient elastography (requires a radiologist or sonographer)</p> <p>Not suitable for point of service</p> <p>Less validated than 1D transient elastography</p> <p>Greater energy absorption by tissue than 1D transient elastography</p>
Shear-wave elastography	<p>Same strengths as point shear-wave elastography techniques</p> <p>Fast imaging permits generation of quantitative elastograms</p> <p>Numerous ROIs may be positioned on the elastograms</p> <p>May reduce sampling variability that can occur with 1D transient elastography and point shear-wave elastography</p>	<p>Same limitations as point shear-wave elastography</p> <p>Limited availability of this ultrasound system</p> <p>Fewer studies on its diagnostic performance for staging liver fibrosis than 1D transient elastography and point shear-wave elastography</p>
MRI		
Magnitude of complex shear modulus	<p>Same hardware and software adopted across MRI vendors, which potentially will provide reproducible results</p> <p>High diagnostic accuracy for advanced fibrosis</p> <p>Robust (feasible in larger patients or those with ascites)</p> <p>Images a larger proportion of the liver, potentially reducing sampling variability for longitudinal monitoring</p> <p>Incremental cost of hardware and software lower than cost of new 1D transient elastography device</p> <p>Low power output and energy absorption by tissues</p>	<p>Quality may be degraded in patients with marked iron deposition</p> <p>Requires postprocessing and offline analysis</p> <p>Limited availability outside of academic centers</p> <p>Some subjectivity in selecting ROIs</p> <p>Additional time required for positioning the transducer</p> <p>Acquisition with different breath-holds</p> <p>Large ROIs not always obtainable because of shear-wave attenuation in normal liver</p>
Complex (storage modulus and loss modulus)	<p>Multifrequency approach permits calculation of elasticity and viscosity</p>	<p>Currently in research domain</p>

es to parametric maps requires solving an inverse problem (i.e., what distribution of stiffness, or related parameter, explains the observed wave patterns). With 2D inversion algorithms, only two-directional components within a slice of the 3D wave propagation are analyzed. With 3D inversion algorithms, a more complete analysis of the full wave motion is possible. Mathematic inversion algorithms currently require simplifying assumptions about tissue properties [45], including that it has a uniform density of 1 g/cm<sup>3</sup> and that it is purely viscoelastic with locally (microscopically) homogeneous, isotropic, and linear mechanical properties. The color elastograms represent the shear modulus with scales of 0–8 kPa and 0–20 kPa. In an advanced implementation, an elastogram confidence mask is automatically created that displays the portions of the elastogram in which the wave data are considered reliable.

### Image Analysis

To obtain a single reportable value from the multislice parametric maps, the MR elastography-generated magnitude images, wave images, and elastogram confidence masks are viewed together. Geographic ROIs are drawn manually on portions of the liver parenchyma with reliable data, while avoiding edges of liver, large blood vessels, and regions with multipath wave interference. Because ROIs are drawn manually, some subjectivity (operator dependence) is unavoidable. Automated analysis techniques are in development; these are expected to reduce operator dependence.

### Parameters Reported

In most publications using a now commercially available implementation of MR elastography, quantitative results have been reported as “shear stiffness” in kilopascals. This is taken to mean the magnitude of the complex modulus, also in kilopascals [46–49]. See example elastograms in Figure 5. Publications using investigational implementations have reported additional parameters, such as storage ( $G'$ ) and loss modulus ( $G''$ ) [39] or elasticity and viscosity, by assuming a Kelvin-Voigt model [50].

**Advantages**—Although numerous investigative teams have developed different MR elastography techniques, using different hardware and software, only one technique is being adopted for clinical implementation by the major MRI scanner manufacturers, which potentially will enable reproducibility of results.

The hardware and software for this technique are produced by Resoundant and are made available by the scanner manufacturers as commercial elastography packages. MR elastography provides a high diagnostic accuracy for advanced fibrosis. This technique is robust, because it is feasible in larger patients or even those with ascites. Compared with ultrasound-based techniques, MR elastography assesses a larger proportion of the liver, which may potentially reduce sampling variability for longitudinal monitoring. The incremental cost of hardware and software is less than the cost of a new 1D transient elastography device but higher than the cost of purchasing shear-wave elastography software for an existing ultrasound system. Power output and energy absorption by tissues are minimal, because the shear waves are generated externally.

**Limitations**—Because of the reliance on gradient-recalled echo sequences, quality in the current commercial implementation may be degraded in patients with iron deposition. Investigational sequences may permit MR elastography measurements even in patients with significant iron deposition. MR elastography requires postprocessing and offline analysis to obtain valid average stiffness measurements. The calculation involves some subjectivity inherent to the selection of the ROIs. MR elastography has limited availability outside of academic centers. Additional time is required for positioning the passive transducer, and the tension with which the transducer is secured is not yet standardized. The transducer causes discomfort in some patients, which may be alleviated by flexible traducers in development. Liver MR elastography is acquired with different breath-holds; if breath-holds are not consistent, this may potentially introduce errors that are not yet well characterized. Finally, shear waves tend to attenuate in normal (soft) livers; consequently, wave propagation may be poor in patients with normal livers, and large ROIs are not always obtainable.

### Comparison of Techniques

The relative strengths and limitations of ultrasound- and MRI-based techniques for staging of liver fibrosis are summarized in Table 4.

### Conclusion

Over the past 2 decades, elastography techniques have evolved significantly from investigational prototypes to clinical tools used for patient care. Depending on the indication (screening, diagnosis, or monitoring of liver fibrosis), different modalities may

be preferred according to their respective strengths and limitations.

Ultrasound elastography techniques are relatively inexpensive, portable, and increasingly available while providing good diagnostic accuracy but may be unreliable in obese patients and those with narrow intercostal spaces. MR elastography offers excellent diagnostic accuracy that probably slightly exceeds that of ultrasound-based techniques, but quality may be degraded in patients with marked iron deposition, and availability remains comparatively limited. In a research setting, MR elastography may become a surrogate reference standard when liver biopsy is either not feasible or acceptable.

### References

1. Sarvazyan AP, Rudenko OV, Swanson SD, Fowlkes JB, Emelianov SY. Shear wave elasticity imaging: a new ultrasonic technology of medical diagnostics. *Ultrasound Med Biol* 1998; 24:1419–1435
2. Sandrin L, Fourquet B, Hasquenoph JM, et al. Transient elastography: a new noninvasive method for assessment of hepatic fibrosis. *Ultrasound Med Biol* 2003; 29:1705–1713
3. Nightingale K, McAleavey S, Trahey G. Shear-wave generation using acoustic radiation force: in vivo and ex vivo results. *Ultrasound Med Biol* 2003; 29:1715–1723
4. Muthupillai R, Lomas DJ, Rossman PJ, Greenleaf JF, Manduca A, Ehman RL. Magnetic resonance elastography by direct visualization of propagating acoustic strain waves. *Science* 1995; 269:1854–1857
5. Tang A, Cloutier G, Szeverenyi NM, Sirlin CB. Ultrasound elastography and MR elastography for assessing liver fibrosis. Part 2. Diagnostic performance, confounders, and future directions. *AJR* 2015; 206(in press)
6. Varghese T. Quasi-static ultrasound elastography. *Ultrasound Clin* 2009; 4:323–338
7. D'Hooge J, Heimdal A, Jamal F, et al. Regional strain and strain rate measurements by cardiac ultrasound: principles, implementation and limitations. *Eur J Echocardiogr* 2000; 1:154–170
8. Naim C, Cloutier G, Mercure E, et al. Characterisation of carotid plaques with ultrasound elastography: feasibility and correlation with high-resolution magnetic resonance imaging. *Eur Radiol* 2013; 23:2030–2041
9. Yoneda M, Suzuki K, Kato S, et al. Nonalcoholic fatty liver disease: US-based acoustic radiation force impulse elastography. *Radiology* 2010; 256:640–647
10. Stein S, Wysession M. *An introduction to seismology, earthquakes, and earth structure*. Malden, MA: Wiley-Blackwell, 2003:512
11. Huwart L, Sempoux C, Vicaut E, et al. Magnetic resonance elastography for the noninvasive staging

- of liver fibrosis. *Gastroenterology* 2008; 135:32–40
12. Nightingale K, Soo MS, Nightingale R, Trahey G. Acoustic radiation force impulse imaging: in vivo demonstration of clinical feasibility. *Ultrasound Med Biol* 2002; 28:227–235
  13. Muller M, Gennisson JL, Deffieux T, Tanter M, Fink M. Quantitative viscoelasticity mapping of human liver using supersonic shear imaging: preliminary in vivo feasibility study. *Ultrasound Med Biol* 2009; 35:219–229
  14. Chen S, Sanchez W, Callstrom MR, et al. Assessment of liver viscoelasticity by using shear waves induced by ultrasound radiation force. *Radiology* 2013; 266:964–970
  15. Bamber J, Cosgrove D, Dietrich CF, et al. EFSUMB guidelines and recommendations on the clinical use of ultrasound elastography. Part 1. Basic principles and technology. *Ultraschall Med* 2013; 34:169–184
  16. Audière S, Angelini ED, Sandrin L, Charbit M. Maximum likelihood estimation of shear wave speed in transient elastography. *IEEE Trans Med Imaging* 2014; 33:1338–1349
  17. Sandrin L, Tanter M, Gennisson JL, Catheline S, Fink M. Shear elasticity probe for soft tissues with 1-D transient elastography. *IEEE Trans Ultrason Ferroelectr Freq Control* 2002; 49:436–446
  18. Catheline S, Thomas JL, Wu F, Fink MA. Diffraction field of a low frequency vibrator in soft tissues using transient elastography. *IEEE Trans Ultrason Ferroelectr Freq Control* 1999; 46:1013–1019
  19. Gennisson JL, Deffieux T, Fink M, Tanter M. Ultrasound elastography: principles and techniques. *Diagn Interv Imaging* 2013; 94:487–495
  20. Sandrin L, Cassereau D, Fink M. The role of the coupling term in transient elastography. *J Acoust Soc Am* 2004; 115:73–83
  21. Kim S, Kang Y, Lee MJ, Kim MJ, Han SJ, Koh H. Points to be considered when applying FibroScan S probe in children with biliary atresia. *J Pediatr Gastroenterol Nutr* 2014; 59:624–628
  22. FibroScan. Probe XL. FibroScan website. www.echosenscorporate.com/en/xl-probe.html. Accessed November 24, 2014
  23. Cosgrove D, Piscaglia F, Bamber J, et al. EFSUMB guidelines and recommendations on the clinical use of ultrasound elastography. Part 2. Clinical applications. *Ultraschall Med* 2013; 34:238–253
  24. Friedrich-Rust M, Ong MF, Martens S, et al. Performance of transient elastography for the staging of liver fibrosis: a meta-analysis. *Gastroenterology* 2008; 134:960–974
  25. Myers RP, Pomier-Layrargues G, Kirsch R, et al. Feasibility and diagnostic performance of the FibroScan XL probe for liver stiffness measurement in overweight and obese patients. *Hepatology* 2012; 55:199–208
  26. Naveau S, Lamouri K, Pourcher G, et al. The diagnostic accuracy of transient elastography for the diagnosis of liver fibrosis in bariatric surgery candidates with suspected NAFLD. *Obes Surg* 2014; 24:1693–1701
  27. de Lédighen V, Vergniol J, Foucher J, El-Hajbi F, Merrouche W, Rigalleau V. Feasibility of liver transient elastography with FibroScan using a new probe for obese patients. *Liver Int* 2010; 30:1043–1048
  28. Friedrich-Rust M, Hadji-Hosseini H, Kriener S, et al. Transient elastography with a new probe for obese patients for non-invasive staging of non-alcoholic steatohepatitis. *Eur Radiol* 2010; 20:2390–2396
  29. Cassinotto C, Lapuyade B, Ait-Ali A, et al. Liver fibrosis: noninvasive assessment with acoustic radiation force impulse elastography—comparison with FibroScan M and XL probes and FibroTest in patients with chronic liver disease. *Radiology* 2013; 269:283–292
  30. Wong GL, Vergniol J, Lo P, et al. Non-invasive assessment of liver fibrosis with transient elastography (FibroScan®): applying the cut-offs of M probe to XL probe. *Ann Hepatol* 2013; 12:570–580
  31. Nightingale K. Acoustic radiation force impulse (ARFI) imaging: a review. *Curr Med Imaging Rev* 2011; 7:328–339
  32. U.S. Food and Drug Administration (FDA). S2000 and S300 Virtual Touch IQ 510(k) submission. FDA website. www.accessdata.fda.gov/cdrh\_docs/pdf13/K130881.pdf. Published March 26, 2013. Accessed November 24, 2014
  33. Friedrich-Rust M, Nierhoff J, Lupsor M, et al. Performance of acoustic radiation force impulse imaging for the staging of liver fibrosis: a pooled meta-analysis. *J Viral Hepat* 2012; 19:e212–e219
  34. Bercoff J, Tanter M, Fink M. Supersonic shear imaging: a new technique for soft tissue elasticity mapping. *IEEE Trans Ultrason Ferroelectr Freq Control* 2004; 51:396–409
  35. Sirli R, Bota S, Sporea I, et al. Liver stiffness measurements by means of supersonic shear imaging in patients without known liver pathology. *Ultrasound Med Biol* 2013; 39:1362–1367
  36. Ferraioli G, Tinelli C, Dal Bello B, Zicchetti M, Filice G, Filice C. Accuracy of real-time shear wave elastography for assessing liver fibrosis in chronic hepatitis C: a pilot study. *Hepatology* 2012; 56:2125–2133
  37. Yoon JH, Lee JM, Joo I, et al. Hepatic fibrosis: prospective comparison of MR elastography and US shear-wave elastography for evaluation. *Radiology* 2014; 273:772–782
  38. Venkatesh SK, Ehman RL. Magnetic resonance elastography of liver. *Magn Reson Imaging Clin N Am* 2014; 22:433–446
  39. Asbach P, Klatt D, Schlosser B, et al. Viscoelasticity-based staging of hepatic fibrosis with multifrequency MR elastography. *Radiology* 2010; 257:80–86
  40. Tse ZT, Janssen H, Hamed A, Ristic M, Young I, Lamperth M. Magnetic resonance elastography hardware design: a survey. *Proc Inst Mech Eng H* 2009; 223:497–514
  41. Yin M, Chen J, Glaser KJ, Talwalkar JA, Ehman RL. Abdominal magnetic resonance elastography. *Top Magn Reson Imaging* 2009; 20:79–87
  42. Sinkus R, Tanter M, Catheline S, et al. Imaging anisotropic and viscous properties of breast tissue by magnetic resonance-elastography. *Magn Reson Med* 2005; 53:372–387
  43. Asbach P, Klatt D, Hamhaber U, et al. Assessment of liver viscoelasticity using multifrequency MR elastography. *Magn Reson Med* 2008; 60:373–379
  44. Klatt D, Asbach P, Rump J, et al. In vivo determination of hepatic stiffness using steady-state free precession magnetic resonance elastography. *Invest Radiol* 2006; 41:841–848
  45. Mariappan YK, Glaser KJ, Ehman RL. Magnetic resonance elastography: a review. *Clin Anat* 2010; 23:497–511
  46. Chen J, Talwalkar JA, Yin M, Glaser KJ, Sanderson SO, Ehman RL. Early detection of nonalcoholic steatohepatitis in patients with nonalcoholic fatty liver disease by using MR elastography. *Radiology* 2011; 259:749–756
  47. Kim D, Kim WR, Talwalkar JA, Kim HJ, Ehman RL. Advanced fibrosis in nonalcoholic fatty liver disease: noninvasive assessment with MR elastography. *Radiology* 2013; 268:411–419
  48. Wang Y, Ganger DR, Levitsky J, et al. Assessment of chronic hepatitis and fibrosis: comparison of MR elastography and diffusion-weighted imaging. *AJR* 2011; 196:553–561
  49. Yin M, Talwalkar JA, Glaser KJ, et al. Assessment of hepatic fibrosis with magnetic resonance elastography. *Clin Gastroenterol Hepatol* 2007; 5:1207.e2–1213.e2
  50. Huwart L, Sempoux C, Salameh N, et al. Liver fibrosis: noninvasive assessment with MR elastography versus aspartate aminotransferase-to-platelet ratio index. *Radiology* 2007; 245:458–466

#### FOR YOUR INFORMATION

A data supplement for this article can be viewed in the online version of the article at: [www.ajronline.org](http://www.ajronline.org).

The reader's attention is directed to Part 2 accompanying this article, titled "Ultrasound Elastography and MR Elastography for Assessing Liver Fibrosis: Part 2, Diagnostic Performance, Confounders, and Future Directions," on the following pages.